Turkish Journal of Computer and Mathematics Education Vol.12 No.13(2021), 2473-2478

Research Article

Continuous Control Set Model Predictive Control for Polysolenoid Linear Motor

Nguyen Hong Quang[a,*], and Nguyen Phung Quang[b]
[a] Thai Nguyen University of Technology, Viet Nam.
[b]Hanoi University of Science and Technology, Viet Nam

Article History: Received: 11 January 2021; Revised: 12 February 2021; Accepted: 27 March 2021; Published online: 4 June 2021

Abstract: In this paper, a model predictive control (MPC) based on the properties of the voltage source inverter is applied to Polysolenoid motors. Polysolenoid motors are a particular type of permanently excited synchronous motor. It has a tubular texture. On the stator of the motor, there are only two windings. Based on the structural characteristics of the motor, the used source is a two-phase voltage source inverter. When considering the voltage supplied to the two windings from the inverter as continuous, the continuous control set model predictive control (CCS-MPC) is developed at the force loop. Simulation results are performed to illustrate the performance of the implemented system.

Keywords: *MPC, CCS-MPC, Polysolenoid, Linear Motor, FOC*.

1. Introduction

The Polysolenoid motor exerts thrust on the moving part to produce reciprocating motion. The working principle of the Polysolenoid motor has been mentioned in [1-12]. Currently, linear motors have been widely used in industry due to the advantages of efficiency, position accuracy, and reduced system weight. Some typical applications using linear motors can be mentioned, such as micro-motor systems [13,14], vehicle power steering systems [15], compressor drive components in industrial refrigeration systems [16], marine system applications [17], magnetic levitation transport applications [18-20], and so on. The control problem for linear motors has always attracted the attention of researchers. In [19-21], the method of speed control using self-tuning PI controller combined with speed estimation technique in the slow-speed region was introduced. Sliding controllers used to deal with the effects of uncertainty were presented in [22-25]. The backstepping control based on Lyapunov's direct method was applied in [26-29]. In [30], the sliding control method combined with the extreme learning machine (ELM) technique drives the position deviation to equilibrium after a finite number of steps. Using the disturbance observer to control the position error of the motor [8,31], the stability of the system is proved by the Lyapunov method. To solve the control problem with an approximate model, the technique of using neurons was implemented in [32,33]. In the above studies, the role of the inverter is considered as a 1:1 transfer function of modulus and phase angle when performing voltage vector modulation on the stator side. This is not satisfactory because the inverter is essentially bound to the modulation limit. In addition, when considering the switching time of the transistor, the vector modulation domain will become very complicated. The MPC used in this case will be based on solving the optimization problem for the objective function to perform the voltage vector modulation of the inverter, taking into account the constraints.

2. Mathetical model

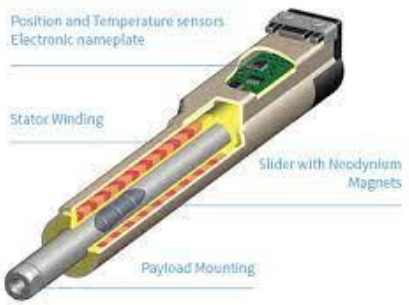

Figure. 1 Polyslenoid motor [4]

The mathematical model of Polysolenoid motor on the dq-coordinate system is as below [12]:

$$\begin{cases} \dfrac{di_{sd}}{dt} = -\dfrac{R_s}{L_{sd}} i_{sd} + \left(\dfrac{2\pi p}{\tau} v\right)\dfrac{L_{sq}}{L_{sd}} i_{sq} + \dfrac{u_{sd}}{L_{sd}} \\ \dfrac{di_{sq}}{dt} = -\dfrac{R_s}{L_{sq}} i_{sq} - \left(\dfrac{2\pi}{\tau} v\right)\dfrac{L_{sd}}{L_{sq}} i_{sd} - \left(\dfrac{2\pi p}{p\tau} v\right)\dfrac{\psi_p}{L_{sq}} + \dfrac{u_{sq}}{L_{sq}} \\ \dfrac{dv}{dt} = \dfrac{2\pi p}{\tau}\left(\psi_p + \left(L_{sd} - L_{sq}\right) i_{sd}\right) i_{sq} - \dfrac{1}{m} F_c \\ \dfrac{dx}{dt} = v \end{cases} \tag{1}$$

From (1), the continuous current model of the Polysolenoid motor on the dq-coordinate system is driven as:

$$\frac{d\mathbf{i}_{dq}}{dt} = \mathbf{A}\mathbf{i}_{dq} + \mathbf{B}\mathbf{u}_{dq} + \mathbf{N}\mathbf{i}_{dq}\omega_e + \mathbf{S}\psi_p\omega_e \tag{2}$$

where

$$\mathbf{i}_{dq}{}^T = \begin{bmatrix} i_d & i_q \end{bmatrix}, \mathbf{u}_{dq}{}^T = \begin{bmatrix} u_d & u_q \end{bmatrix}$$

$$\mathbf{A} = \begin{bmatrix} -\dfrac{R_s}{L_d} & 0 \\ 0 & -\dfrac{R_s}{L_q} \end{bmatrix}, \mathbf{B} = \begin{bmatrix} \dfrac{1}{L_d} & 0 \\ 0 & \dfrac{1}{L_q} \end{bmatrix}, \mathbf{N} = \begin{bmatrix} 0 & \dfrac{L_q}{L_d} \\ -\dfrac{L_d}{L_q} & 0 \end{bmatrix}, \mathbf{S} = \begin{bmatrix} 0 \\ -\dfrac{1}{L_q} \end{bmatrix}$$

3.Control design

From the continuous current model, the discrete-time current model of the stator is obtained as below:

$$\mathbf{i}_{dq}(k+1) = \mathbf{\Phi}\mathbf{i}_{dq}(k) + \mathbf{H}\mathbf{u}_{dq}(k) + \mathbf{h}\psi_p \tag{3}$$

where

$$\mathbf{\Phi} = \mathbf{I} + T_s\mathbf{A} + T_s\mathbf{N}\omega_e(k) = \begin{bmatrix} \Phi_{11} & \Phi_{12} \\ \Phi_{21} & \Phi_{22} \end{bmatrix} = \begin{bmatrix} 1 - T_s R_s / L_d & T_s L_q \omega_e(k) / L_d \\ -T_s L_d \omega_e(k) / L_q & 1 - T_s R_s / L_q \end{bmatrix}$$

$$\mathbf{H} = T_s\mathbf{B} = \begin{bmatrix} H_{11} & 0 \\ 0 & H_{22} \end{bmatrix} = \begin{bmatrix} T_s / L_d & 0 \\ 0 & T_s / L_q \end{bmatrix}, \mathbf{h} = \begin{bmatrix} h_1 \\ h_2 \end{bmatrix} = \begin{bmatrix} 0 \\ -T_s\omega_e(k) / L_q \end{bmatrix}$$

in which, T_s is the sampling time of the current.

Based on the discrete-time model, a predictive model is built with $\mathbf{i}_{dq}^{est}(k+i)$ is the predicted current value at the next i-th samples. Using the discrete-time model (3), we have:

$$\mathbf{i}_{dq}^{est}(k+i+1|k) = \mathbf{\Phi}\mathbf{i}_{dq}^{est}(k+i|k) + \mathbf{H}\bar{\mathbf{u}}_{dq}(k+i) + \mathbf{h}\psi_p \tag{4}$$

where $\mathbf{i}_{dq}^{est}(k) = \mathbf{i}_{dq}(k)$ is at the current sample k ; $\bar{\mathbf{u}}_{dq}(k+i)$ denotes the control signal that need to be determined at at the next i-th samples. The intended use of $\bar{\mathbf{u}}_{dq}$ is to distinguish actual control signals applied to the system, $\mathbf{u}_{dq}(k), \mathbf{u}_{dq}(k-1)$, … With a prediction range N_p, the MPC solves optimal problem with control voltage vectors $\bar{\mathbf{u}}_{dq}(k) = \mathbf{u}_{dq}(k), \bar{\mathbf{u}}_{dq}(k+1), ..., \bar{\mathbf{u}}_{dq}(k+N_p-1)$ as variables.

The selected objective function has the following quadratic form:

$$J = \sum_{i=1}^{N_p} \left[\left(\mathbf{i}_{dq}^{ref} - \mathbf{i}_{dq}^{est}\left(k+i \mid k\right) \right)^T \mathbf{Q} \left(\mathbf{i}_{dq}^{ref} - \mathbf{i}_{dq}^{est}\left(k+i \mid k\right) \right) \right] \tag{5}$$

where $\mathbf{Q} = diag\left(\begin{bmatrix} \lambda_d & 1 \end{bmatrix}\right)$ is a positive definite diagonal matrix, the coefficient λ_d represents the weight of the current deviation from $\left|i_d^{ref} - i_d\right|$ to $\left|i_q^{ref} - i_q\right|$ in the objective function J, $\mathbf{i}_{dq}^{ref}$ is the reference from the output of the speed controller. Due to the fast kinematics of the current control loop, the prediction range is chosen to be small in order to reduce the computation cost in the problem (5) and ensure the performance of the controller. In addition, in industrial applications, the sampling time of the current loop is much faster than that of the speed loop. Combining the above reasons, we can consider the speed and angular position of the motor to be constant during one sampling cycle resulting in $\mathbf{i}_{dq}^{ref}$ is a constant in Equation (5).

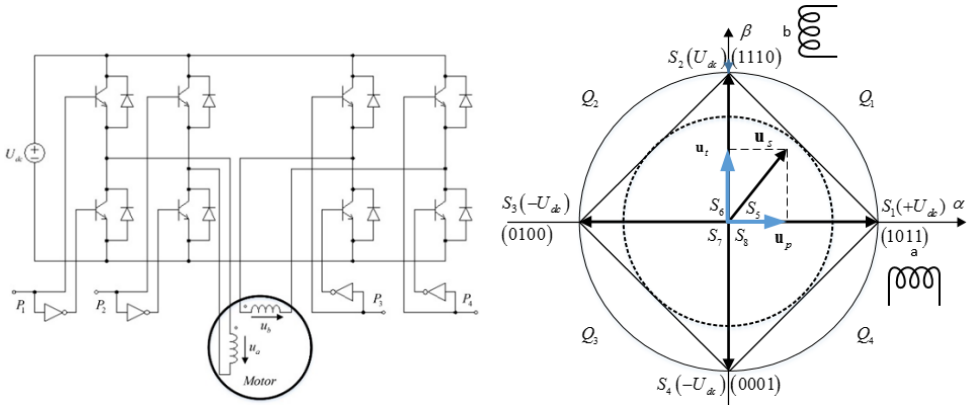

Figure.2 Modulation plane on αβ-coordinate system using CCS-MPC.

The modulation plane on the αβ-coordinate system using CCS-MPCis depicted in Figure.2Condition for A to be in the modulation domain is:

$$\mathbf{A}_{con}\mathbf{u}_s < \mathbf{B}_{con} \tag{6}$$

where $\mathbf{A}_{con} = \begin{bmatrix} 1 & 1 \\ 1 & -1 \\ -1 & 1 \\ -1 & -1 \end{bmatrix}$; $\mathbf{B}_{con} = \begin{bmatrix} 1 \\ 1 \\ 1 \\ 1 \end{bmatrix}$.

From the constraint of $\bar{\mathbf{u}}_s$, we obtain the constraint of $\bar{\mathbf{u}}_{dq}$ as below:

$$\mathbf{A}_{con}\mathbf{R}^{-1}\bar{\mathbf{u}}_{dq}\left(k+i\right) < \mathbf{B}_{con} \tag{7}$$

where $\mathbf{R} = \begin{bmatrix} \cos(\theta) & -\sin(\theta) \\ \sin(\theta) & \cos(\theta) \end{bmatrix}$

Accordingly, the optimization problem (5) with the cost function J can be converted into a quadratic form, with $\bar{\mathbf{u}}_{dq}\left(k\right) = \mathbf{u}_{dq}\left(k\right)$ is the the optimal variable, as below:

$$\begin{aligned} \min_{\bar{u}_{dq}(k)} \; & J = \bar{u}_{dq}\left(k\right)^T \left(H^T Q H\right) \bar{u}_{dq}\left(k\right) \\ & 2\left(\Phi i_{dq}\left(k\right) + h\psi_p - i_{dq}^{ref}\right)^T Q H \bar{u}_{dq}\left(k\right) + C \end{aligned} \tag{8}$$

$$\mathbf{A}_{con}\mathbf{R}^{-1}\bar{\mathbf{u}}_{dq}\left(k\right) < \mathbf{B}_{con}$$

where C is a component that depends only on the current state and the current velocity and does not depend on $\mathbf{u}_{dq}\left(k\right)$.

4.Simulation results

The motor parameters are described in Table. 1.

Table.1. Motor parameters

Motor parameters	Symbol	Value	Unit
d-axis stator inductance	L_{sd}	1.4	mH
q-axis stator inductance	L_{sq}	1.4	mH
Stator resistance	R_s	10.3	Ω
Rotor flux	ψ_p	0.035	Wb
Number of pole pairs	z_p	2	
Pole step	τ_p	0.02	m

Simulation is performed with the current sampling time $T_i = 100(\mu s)$ .Response of the CCS-MPC current regulator to a change in the current loop reference value.

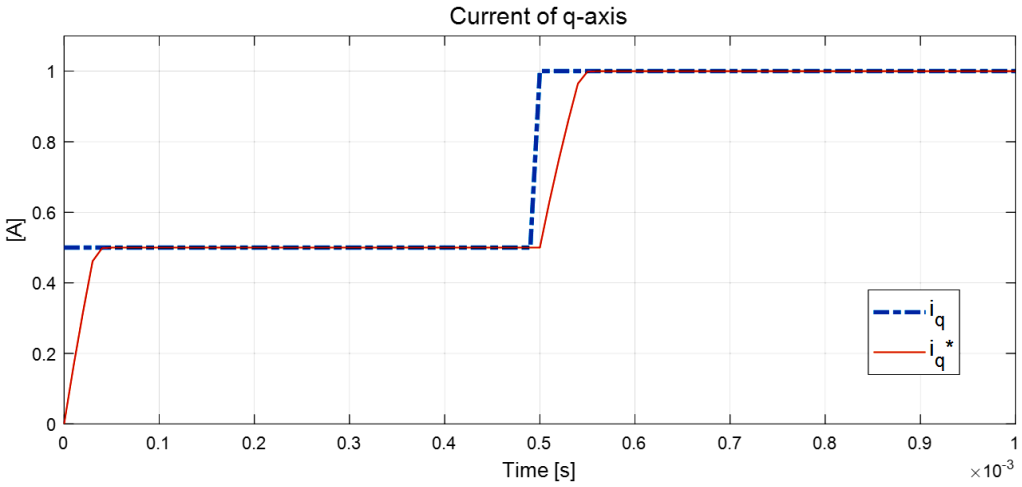

Figure.3 Current response iq

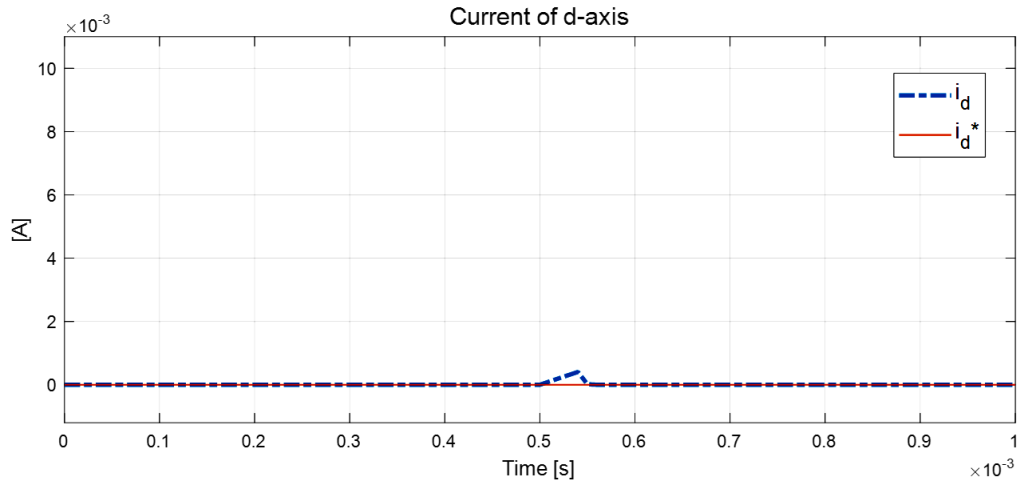

Figure. 4Current response id

Comments: At the time of changing the q-axis reference current value (Figure 4, Figure 5), the iq current value reaches the reference value, the id current is also returned to zero. The id is affected but not significantly, and this is an acceptable value. To drive the value of the d-axis current closer to zero, we change the weighted value λ_d. We see that the controller design has performed demultiplexing between the two d-, q- axes.

5. Conclusion

The CCS-MPC control method applied to Poysolenoid motors has promoted its efficiency by decoupling the currents on the two d-, q- axes corresponding to the flux generation and thrust axes. In this paper, since the sampling time of the force loop is extremely small, $T_i = 100(\mu s)$, the prediction range is limited. When using the CCS-MPC method, the processing capacity of the microcontroller plays a decisive role in the responsibility of the system. For higher power motors, the CCS-MPC method will be a very suitable choice. Since the system has a large electromagnetic time constant ($T_u = L_u/R_u$), a larger sampling period will be chosen. That will balance the criteria of the processing power of the microcontroller and the quality of the system. We can more easily select a processor to reduce costs as well as have more choices in the popular processors available to integrate into the system.

Acknowledgments

This research was funded by Thai Nguyen University of Technology, No. 666, 3/2 street, Thai Nguyen, Viet Nam.

References

[1] Ausderau, D. (2004). *Polysolenoid-Linearantrieb mit genutetem Stator* (Doctoral dissertation, ETH Zurich).
[2] Gieras, J. F. (2018). Linear Electric Motors. In *Electric Power Generation, Transmission, and Distribution: The Electric Power Engineering Handbook* (pp. 34-1). CRC Press.
[3] Boldea, I., Tutelea, L. N., Xu, W., & Pucci, M. (2017). Linear electric machines, drives, and MAGLEVs: an overview. *IEEE Transactions on Industrial Electronics*, *65*(9), 7504-7515.
[4] LinMot Company Home Page: Products, Linear Motors. Available online: https://linmot.com/products/ linear-motors/ (accessed on 1 March 2020).
[5] Nguyen, Q. H., Dao, N. P., Nguyen, T. T., Nguyen, H. M., Nguyen, H. N., & Vu, T. D. (2016). Flatness based control structure for polysolenoid permanent stimulation linear motors. *SSRG International Journal of Electrical and Electronics Engineering*, *3*(12), 31-37.
[6] Quang, N. H. (2017). Multi parametric programming based model predictive control for tracking control of polysolenoid linear motor. *Special issue on Measurement, Control and Automation*, *19*, 31-37.
[7] Quang, N. H., Quang, N. P., & Hien, N. N. (2020). On tracking control problem for polysolenoid motor model predictive approach. *International Journal of Electrical & Computer Engineering (2088-8708)*, *10*(1).
[8] Nguyen, H. Q. (2020, March). Observer-Based Tracking Control for Polysolenoid Linear Motor with Unknown Disturbance Load. In *Actuators* (Vol. 9, No. 1, p. 23).
[9] Nam, D. P., Quang, N. H., Hung, N. M., & Ty, N. T. (2017, July). Multi parametric programming and exact linearization based model predictive control of a permanent magnet linear synchronous motor. In *2017 International Conference on System Science and Engineering (ICSSE)* (pp. 743-747). IEEE.
[10] Ty, N. T., Hung, N. M., Nam, D. P., & Quang, N. H. (2018). A Laguerre model-based model predictive control law for permanent magnet linear synchronous motor. In *Information Systems Design and Intelligent Applications* (pp. 304-313). Springer, Singapore.
[11] Quang, N. H., Quang, N. P., Nam, D. P., & Binh, N. T. (2019). Multi parametric model predictive control based on laguerre model for permanent magnet linear synchronous motors. *International Journal of Electrical and Computer Engineering (IJECE)*, *9*(2), 1067-1077.
[12] Nguyen, H. Q., Nguyen, P. Q., Nguyen, N. H., & Nguyen, T. B. (2018). Min max model predictive control for polysolenoid linear motor. *International Journal of Power Electronics and Drive Systems*, *9*(4), 1666.
[13] Lu, H., Zhu, J., & Guo, Y. (2005). Development of a slotless tubular linear interior permanent magnet micromotor for robotic applications. *IEEE transactions on magnetics*, *41*(10), 3988-3990.
[14] Lu, H., Zhu, J., & Guo, Y. (2005, December). A permanent magnet linear motor for micro robots. In *2005 International Conference on Power Electronics and Drives Systems* (Vol. 1, pp. 590-595). IEEE.
[15] Akhondi, H., & Milimonfared, J. (2009). Design and optimization of tubular permanent magnet linear motor for electric power steering system. *Journal of Asian Electric Vehicles*, *7*(2), 1283-1289.
[16] Wang, J., Howe, D., & Lin, Z. (2009). Design optimization of short-stroke single-phase tubular permanent-magnet motor for refrigeration applications. *IEEE Transactions on Industrial electronics*, *57*(1), 327-334.

[17] Pirisi, A., Gruosso, G., & Zich, R. E. (2009, March). Novel modeling design of three phase tubular permanent magnet linear generator for marine applications. In *2009 International Conference on Power Engineering, Energy and Electrical Drives* (pp. 78-83). IEEE.

[18] Seok, J. K., Lee, J. K., & Lee, D. C. (2006). Sensorless speed control of nonsalient permanent-magnet synchronous motor using rotor-position-tracking PI controller. *IEEE Transactions on Industrial Electronics*, *53*(2), 399-405.

[19] Huang, S., Ching, T. W., Li, W., & Deng, B. (2018, June). Overview of linear motors for transportation applications. In *2018 IEEE 27th International Symposium on Industrial Electronics (ISIE)* (pp. 150-154). IEEE.

[20] Wang, K., Ge, Q., Shi, L., Li, Y., & Zhang, Z. (2017, September). Development of ironless Halbach permanent magnet linear synchronous motor for traction of a novel maglev vehicle. In *2017 11th International Symposium on Linear Drives for Industry Applications (LDIA)* (pp. 1-5). IEEE.

[21] Wang, H., Li, J., Qu, R., Lai, J., Huang, H., & Liu, H. (2018). Study on high efficiency permanent magnet linear synchronous motor for maglev. *IEEE Transactions on Applied Superconductivity*, *28*(3), 1-5.

[22] Sun, G., Wu, L., Kuang, Z., Ma, Z., & Liu, J. (2018). Practical tracking control of linear motor via fractional-order sliding mode. *Automatica*, *94*, 221-235.

[23] Du, H., Chen, X., Wen, G., Yu, X., & Lü, J. (2018). Discrete-time fast terminal sliding mode control for permanent magnet linear motor. *IEEE Transactions on Industrial Electronics*, *65*(12), 9916-9927.

[24] Yang, C., Ma, T., Che, Z., & Zhou, L. (2017). An adaptive-gain sliding mode observer for sensorless control of permanent magnet linear synchronous motors. *IEEE Access*, *6*, 3469-3478.

[25] Sun, G., & Ma, Z. (2017). Practical tracking control of linear motor with adaptive fractional order terminal sliding mode control. *IEEE/ASME Transactions on Mechatronics*, *22*(6), 2643-2653.

[26] Sun, G., Wu, L., Kuang, Z., Ma, Z., & Liu, J. (2018). Practical tracking control of linear motor via fractional-order sliding mode. *Automatica*, *94*, 221-235.

[27] Du, H., Chen, X., Wen, G., Yu, X., & Lü, J. (2018). Discrete-time fast terminal sliding mode control for permanent magnet linear motor. *IEEE Transactions on Industrial Electronics*, *65*(12), 9916-9927.

[28] Yang, C., Ma, T., Che, Z., & Zhou, L. (2017). An adaptive-gain sliding mode observer for sensorless control of permanent magnet linear synchronous motors. *IEEE Access*, *6*, 3469-3478.

[29] Sun, G., & Ma, Z. (2017). Practical tracking control of linear motor with adaptive fractional order terminal sliding mode control. *IEEE/ASME Transactions on Mechatronics*, *22*(6), 2643-2653.

[30] Shao, K., Zheng, J., Wang, H., Xu, F., Wang, X., & Liang, B. (2021). Recursive sliding mode control with adaptive disturbance observer for a linear motor positioner. *Mechanical Systems and Signal Processing*, *146*, 107014.

[31] Shao, K., Zheng, J., Wang, H., Xu, F., Wang, X., & Liang, B. (2021). Recursive sliding mode control with adaptive disturbance observer for a linear motor positioner. *Mechanical Systems and Signal Processing*, *146*, 107014.

[32] Huang, C., & Liu, B. (2019). New studies on dynamic analysis of inertial neural networks involving non-reduced order method. *Neurocomputing*, *325*, 283-287.

[33] Huang, C., & Zhang, H. (2019). Periodicity of non-autonomous inertial neural networks involving proportional delays and non-reduced order method. *International Journal of Biomathematics*, *12*(02), 1950016.